ROYAL SOCIETY
OF CHEMISTRY

PAPER

Check for updates

The synthesis of polymeric dyes based on waterborne polyurethane: a reaction kinetics study using UV absorption spectroscopy

Jun Zhu,[ab] Jie Li,[a] Chao Sang[a] and Yunjun Luo (ID) *[ab]

Waterborne polyurethane (WPU) based polymeric dyes with anthraquinone chromophores were developed to realize coloring textiles and improve color fastness. The preparation of polymeric dyes through the reaction of 1,4-diamino-2,3-diphenoxyanthraquinone (DV26) and NCO-terminated prepolymer was monitored *via* UV absorption spectroscopy. With the progress of the reaction, the intensity of the absorption peak of the primary amine group at 586 nm decreased as a function of reaction time. Thus, the conversion of DV26 at different times and the reaction end point could be determined. The reaction mechanism corresponded to an autocatalytic reaction equation, basically. In addition, the results of performance tests showed that the polymeric dyes exhibited good emulsion stability, ultra-low migration percentages, good water resistance and excellent thermal stability. Moreover, the application properties of DWPU on coated polyester fabrics were satisfactory.

1. Introduction

As the demand for reducing volatile organic compounds (VOCs) and hazardous air pollutants emissions has increased, water-borne polyurethane (WPU) has become an attractive choice due to its excellent mechanical properties, chemical resistance, adhesion and low VOCs.[1–3] As a result, WPU had been widely used in coating, adhesives, elastomers and many other fields. Generally, WPU resin is either physically mixed with dye and pigment pastes or colored by post-colorization to obtain color coatings with better application performance.[4] However, it was inevitably necessary to add some auxiliaries into WPU to enhance the compatibility of multiple phases, which would greatly deteriorate the stability and uniformity of the emulsions.[5] In addition, the preparation of a color paste was usually cumbersome and the application process was very complicated and time consuming.[6,7] Besides, the weak physical interaction between WPU and dyes would result in poor migration resistance, durability and color fastness of colored coatings. These short-comings had greatly limited the application scope of color coatings. Fortunately, these problems could be addressed by the application of novel WPU based polymeric dyes.[8–10]

A WPU based polymeric dye is a kind of self-colored WPU whose dye chromophore is chemically bonded to the main or side chains *via* a chemical reaction.[11–13] Therefore, a polymeric dye could exhibit properties of both dyes and WPU, such as chromaticity, photo absorption, transparency, solvent resistance, film-forming and heat resistance.[14,15] Additionally, polymeric dyes would not be absorbed by the skin on account of their large molecular weight and chemical stability.[16] Thus, polymeric dyes could meet the demands of the modern printing and dyeing industry for power saving, environmental protection and easy processing sequences. Moreover, they could also offer the advantages of improved dyeing fastness, low dye dosage needed and superior security.[17–19] WPU based polymeric dyes have attracted increasing interest from researchers recently.[20]

In general, WPU based polymeric dyes are synthesized through a chemical reaction between isocyanate groups (NCO) in the polyurethane prepolymer and some reactive groups (hydroxy or amino groups) in the chromophore.[21] The reaction was one of the key factors affecting the performance of the polymeric dye.[22] Nevertheless, few studies have reported the monitoring of the reaction of chromophores and prepolymers. Therefore, in order to optimize the synthetic conditions and improve the properties of the polymeric dye, the reaction kinetics mechanisms must be studied thoroughly. In general, titration or IR spectroscopy were commonly used to determine the content of NCO of WPU, thereby monitoring the reaction degree.[23,24] However, it was inappropriate to determine the content of NCO by traditional methods in a WPU based polymeric dye, because chromophores usually had dark colors and were incompatible with a WPU prepolymer.

Fortunately, we found that the reactive groups of chromophores had obvious ultraviolet characteristic absorption. After reaction

[a] *School of Materials Science and Engineering, Beijing Institute of Technology, Beijing 100081, China. E-mail: yjluo@bit.edu.cn; Tel: +86 10 68913698*

[b] *Key Laboratory of High Energy Density Materials of Ministry of Education, Beijing Institute of Technology, Beijing, 100081, China*

with NCO, the absorption peak intensity of the reactive groups would be weakened significantly or disappear finally. Therefore, the conversion of chromophores could be determined by the change of peak intensity. By measuring the UV absorption spectrum of the WPU prepolymer at different times, the reaction kinetics could be studied and the synthesis routine could be optimized. Moreover, the kinetic mechanism function, rate constant and related kinetic parameter could also be obtained.

Herein, a series of WPU based polymeric dyes with 1,4-diamino-2,3-diphenoxyanthraquinone (Disperse Violet 26, DV26) as the chromophore was prepared. The reaction kinetics of DV26 with the NCO-terminated prepolymer were monitored by UV absorption spectroscopy for the first time, and the kinetic parameters were calculated by Arrhenius law and the Eyring equation. The kinetic parameters would be helpful to adjust the WPU curing conditions, such as reaction time, temperature, and so on. The polymeric dye prepared through the optimized process showed excellent properties and had good application performances on polyester fabrics.

2. Experimental section

2.1 Materials

Isophorone diisocyanate (IPDI), 2,2-dimethylol propionic acid (DMPA), trimethylamine (TEA), dibutyltin dilaurate (DBTDL), chloroform-d (CDCl$_3$) and 1,4-butanediol (BDO) were both supplied by Aladdin (Shanghai) Co., Ltd. 2-Butanone (MEK) and ethylenediamine (EDA) were purchased from Beijing Chemical Works. Poly (propylene glycol) with a molecular weight of 1000 (PPG1000) was purchased from Dawson International Inc., Buffalo Grove, IL, USA. 1,4-Diamino-2,3-diphenoxy-anthraquinone (Disperse Violet 26, DV26) was supplied by LANXESS Chemical (China) Co., Ltd. PPG1000 and DMPA were vacuum-dried at 100 °C for 12 h prior to use to remove water. IPDI, DBTDL, EDA and DV26 were used as received. TEA and MEK were dried with KOH and CaSO$_4$, respectively, and then purified by distillation under reduced pressure. Polyester fabric and thickening agent 601H were supplied by Zhejiang Transfar Co. Ltd and were used as received.

2.2 Preparation of DWPU emulsions

IPDI, PPG and three drops of DBTDL were added into a dry three-necked flask equipped with a mechanical stirrer, a thermocouple and a reflux condenser, and were heated at 85 °C for 1 h. Subsequently, the reaction was performed at the same temperature for 2.5 h after adding DMPA. After that, the temperature was reduced to 70 °C, then DV26 was added and reacted for 3 h. Additionally, MEK was added to reduce the viscosity. TEA (equal molar ratio as DMPA) was added for neutralization and stirred for 30 min at 40 °C to form NCO-terminated polyurethane. At last, water and EDA were added with a high shearing speed (3000 rpm) to emulsify the solution for 30 minutes. Finally, DWPU emulsion with a solid content of 30 wt% was obtained. Scheme 1 shows a schematic diagram of the synthesis of the

DWPU emulsions. The contents of the components are presented in Table 1. Samples were prepared and named D$_x$WPU and DWPU-y, where x refers to the percentage content of DV26 and y represents the reaction temperature of DV26. DWPU-25 was obtained by physically blending DV26 with WPU at 25 °C.

2.3 Preparation of coated polyester fabrics

A thickened emulsion (601H, 2.5 wt%) was added into DWPU emulsions and stirred for 5 min at 1500 rpm. Subsequently, the samples were evenly coated on the polyester fabric which was fixed by a needle plate. At last, several polyester fabrics coated with DWPUs were obtained by drying the fabrics at 170 °C for 60 seconds.

2.4 Characterization

Fourier transform infrared spectroscopy (FTIR). The FTIR spectra of WPU films were measured by Nicolet 8700 Fourier transformed infrared spectroscopy (Thermo Nicolet Corporation, Waltham, MA, USA). Measurements were carried out in the wavenumber range of 4000–400 cm^{-1} at a 4.0 cm^{-1} resolution over 64 scans.

Proton nuclear magnetic resonance spectroscopy (^{1}H NMR). The ^{1}H-NMR spectra of DV26 and DWPU were measured by an Avance III HD 400 MHz Instrument (Bruker Co., Germany) with CDCl$_3$ as the solvent and tetramethylsilane as the internal standard.

Particle size. The average particle size and the zeta potential of the emulsion were measured by a Nanosizer (Malvern zetasizer Nano ZS90, Malvern Instruments Ltd., Malvern, UK).

Centrifugal stability. The DWPU emulsion was placed in a centrifuge tube and centrifuged at 4000 rpm for 15 minutes. If no sediment was observed at the bottom of the tube after centrifugation, the emulsion had a storage stability period of more than 6 months.

UV-vis absorption spectra. The UV absorbance of DWPUs was measured using a UV-visible spectrophotometer (U-3010, Hitachi Limited, Japan) at room temperature in the wavelength range from 200 nm to 800 nm. The scanning speed was 300 nm min^{-1}. The NCO-terminated WPU prepolymer was dissolved in MEK with the same concentration (4×10^{-5} mol L^{-1}) and its UV absorption spectrum was measured to study the reaction kinetics. The optical path length of the light beam through the material sample was 10 mm.

Thermogravimetric analysis (TGA). The thermogravimetric measurement and char yield of the DWPU films were measured with a thermogravimetric analyzer (Switzerland Mettler TGA/DSC differential thermal scanners, Mettler-Toledo International Inc., Zurich, Switzerland). The samples ranging from 5–10 mg in weight were heated from 30 to 600 °C with a 10 °C min^{-1} heating and under a nitrogen atmosphere (20 mL min^{-1}).

Differential scanning calorimetry (DSC). The DSC curves of the DWPU films were measured by Mettler Toledo DSC (Mettler-Toledo Co. Ltd., Zurich, Switzerland) at a constant heating rate of 10 °C min^{-1} from −100 °C to 140 °C under N$_2$ atmosphere.

Water absorption. The DWPU films were cut into 20 mm × 20 mm pieces and weighed (m_0), then soaked in deionized

Scheme 1 The synthesis route to DWPU.

Table 1 The components of DWPU samples

Sample	IPDI/g	PPG/g	OP550/g	DV26/g	DMPA/g	TEA/g	EDA/g
WPU	28.97	40	0	0	4.02	3.03	1.95
D_1WPU	28.97	40	0	0.8	4.02	3.03	1.95
D_2WPU	28.97	40	0	1.6	4.02	3.03	1.95
D_3WPU	28.97	40	0	2.4	4.02	3.03	1.95
D_4WPU	28.97	40	0	3.2	4.02	3.03	1.95
DWPU-y	28.97	40	0	1.6	4.02	3.03	1.95

water at room temperature for 24 h. The water on the surface of the films was wiped off with a piece of filter paper and weighed (m). The water absorption was calculated by the formula as follows:

$$\text{Water absorption} = \frac{m - m_0}{m_0} \times 100\%$$

where m_0 represents the initial mass of DWPU film and m represents the mass after soaking.

Gel permeation chromatography (GPC). The molecular weights and polydispersity index (PDI) of the DWPU films were obtained using GPC (LC-20A, Shimadzu) at 25 °C using THF as the mobile phase and a flow rate of 1 mL min^{-1}. The raw data were calibrated using universal calibration with polystyrene standards.

Scanning electron microscopy (SEM). The SEM micrographs of the polyester fabric surface were measured by a Hitachi SU8020 field emission scanning electron microscope (Hitachi Co., Japan) under a 10 kV accelerating voltage. Samples were mounted with carbon tape on aluminum stubs and then sputter-coated with gold (10 nm) to make them conductive prior to SEM observation.

Thermal migration properties[25]. DWPU emulsion was coated on the glass sheet evenly to form a film (Scheme 2). After the DWPU film was dried, region a was covered with a glass dish tightly, while region b was left uncovered. The samples were then placed in an oven at 60 °C for 48 h. The films of regions a and b were respectively dissolved in ethanol with the same concentration, and then the UV-vis spectra of the solutions were measured. M_P was calculated as follows:

$$M_P = \frac{A_a - A_b}{A_a} \times 100\%$$

Scheme 2 The measurement of the migration properties.

where A_a and A_b were the absorbance of the maximum absorption wavelength in regions a and b, respectively.

Color property. The color property of coated polyester fabrics was measured by SF-300 colorimeter (Datacolor, USA). A black tube and a whiteboard were used to calibrate the instrument. The resulting color parameters included the K/S value, L^*, a^*, b^*, c^* and h^0, which represent the apparent color yield, brightness, green-red color axis, yellow-blue color axis, saturation and hue respectively.

Color fastness. The rubbing fastness was tested using LFY-304 crocking fastness tester (Wenzhou Textile Research Institute, China). The washing fastness was tested using WF-517 washing fastness tester (Wenzhou Textile Research Institute, China).

3. Results and discussion

3.1 The UV absorption spectrum of DWPU

Fig. 1 showed the UV absorption spectra of DWPUs reacted at different temperatures. The absorption peaks at 254 nm and 315 nm were caused by the n–π* and p–π* electronic transition of benzoquinone in DV26. The absorption band at 500–600 nm resulted from the π–π* electronic transition between the acetophenone chromophores and the primary amino groups of DV26.[26] With the reaction temperature of DV26 increasing, the intensity of the absorption band at 500–600 nm decreased gradually. However, DWPU only had an absorption peak at

506 nm when the temperature was higher than 70 °C. The intensity of the absorption band at 500–600 nm decreased as DV26 reacted with the NCO-terminated WPU prepolymer, which was attributed to the decrease of the primary amino groups. When all the primary amine groups of DV26 were reacted, there was only an absorption peak at 506 nm, which was attributed to the π–π* electronic transition between the acetophenone chromophores and the secondary amine. The benzoquinone did not take part in the reaction, so the absorption peaks at 254 and 315 nm did not change.

3.2 UV absorption spectra and reaction kinetics

As the primary amine in DV26 was consumed and the benzoquinone remained unchanged, it was reasonable and feasible to study the reaction kinetics by monitoring the absorbance changes of the UV absorption peak at 586 nm against the reference peak at 255 nm. To investigate the reaction rate of DV26 at different temperatures, the UV absorption spectra of the DWPU prepolymers reacted at 50, 60, 70 and 80 °C were measured. The UV absorption spectra of the DWPU prepolymers at 70 °C (Fig. 2) showed that the intensity of the absorption peak at 586 nm decreased gradually with prolonged reaction time. Finally, the absorption peak at 586 nm disappeared. The same trend can be observed in their UV absorption spectra at other temperatures.

According to the Beer–Lambert law,[27,28] the relationship between the concentration of the group and the absorbance was in accordance with the following eqn (1):

$$A = \varepsilon \cdot c \cdot l \qquad (1)$$

where A was the absorbance, ε was the extinction coefficient of the group, l was the path length of the light beam through the material sample, c was the concentration of the group. The relationship between conversion α and absorbance A could be identified by eqn (2):

$$\alpha = \frac{C_0 - C_t}{C_0} = \frac{C_0/C^0 - C_t/C^t}{C_0/C^0} = 1 - \frac{C_t/C^t}{C_0/C^0} = 1 - \frac{A_t/A^t}{A_0/A^0} \quad (2)$$

where C_0 was the initial concentration of primary amine, C_t was the concentration of primary amine at time t, C^0 was the initial

Fig. 1 The UV absorption spectra of DWPUs.

Fig. 2 The UV absorption spectra of DWPU prepolymers reacted at 70 °C.

Fig. 3 The conversion curves of DV26 *versus* time at different temperatures.

concentration of reference group (benzoquinone), C^t was the concentration of reference group at time t. A^t and A_t were the intensity of the absorption peak at 255 nm and 586 nm, respectively.

According to eqn (2), the real-time conversion of DV26 at different temperatures could be calculated by the changes of UV absorption spectra of DWPU prepolymers (Fig. 3). The results showed that the conversion rate of DV26 increased with the reaction time at the same temperature, and reached a maximum finally. In addition, the higher the reaction temperature, the higher the conversion of DV26 at the same time, which indicated that the reaction rate of DV26 accelerated with increasing temperature. After the reaction proceeded for 2.5 h at 70 °C, the conversion rate reached a maximum and would not change significantly even when the time was extended.

Therefore, the end point of the reaction could be determined by the changes of the conversion rate, thereby realizing the optimization of the synthesis. Other than that, the reaction mechanism could be inferred by fitting the kinetic mechanism function and then using it to explain the reaction type and molecular diffusion modes.[29–31]

3.3 Analysis of kinetic models

In general, the kinetic model of chemical reactions can be divided into the nth level model, the autocatalytic model and Kamal model. The reaction kinetic equations were as follows:[32,33]

nth level model:

$$d\alpha/dt = A \cdot (1 - \alpha)^n \cdot e^{(E_a/RT)} \tag{3}$$

Autocatalytic model:

$$d\alpha/dt = A \cdot \alpha^m \cdot (1 - \alpha)^n \cdot e^{(E_a/RT)} \tag{4}$$

Kamal model:

$$d\alpha/dt = (k_1 + k_2\alpha^m) \cdot (1 - \alpha)^n \tag{5}$$

where m and n were reaction order, A was the frequency factor, k_1 and k_2 were reaction rate constants, E_a was the activation energy, T was the temperature, and R was the universal gas constant, 8.314 J (mol K)$^{-1}$. The rate constant was used in the model to predict the progress of the reaction process at different temperatures. Table 2 showed parts of the kinetic mechanism functions.

Thermodynamic parameters were calculated according to the Arrhenius law and Eyring equation by plotting:

$$k = A \cdot e^{(E_a/RT)} \tag{6}$$

$$\ln k = \ln A - \frac{E_a}{RT} \tag{7}$$

$$\ln \frac{k}{T} = -\frac{\Delta H}{RT} + \frac{\Delta S}{R} + \ln \frac{R}{Nh} \tag{8}$$

where N was Avogadro's constant ($N = 6.02 \times 10^{23}$) and h was Planck's constant ($h = 6.62 \times 10^{-34}$ J s). Other authors had investigated the kinetics of the reaction between reactive groups and isocyanates by using these mechanism functions.[34] The k values at different temperatures could be obtained by applying the mechanism function to the reaction kinetic models. The curves of conversion rate calculated from kinetic mechanism functions were linearly fitted with reaction time. The results of the linear fitting are shown in Fig. 4 and the slope of the linear was the reaction rate constant k. The fitted correlation coefficient r and the slope of the line k were shown in Table 3. It could be seen that, the fitted correlation coefficient r at different temperatures was bigger than 0.995, so the linear correlation between time and the integral form of the autocatalytic reaction mechanism functions was good.

As is known to all, the activation energy of the polymerization reaction is calculated from the Arrhenius equation [eqn (7)], while the activation enthalpy and entropy of the polymerization reaction are calculated from the Eyring equation [eqn (8)]. The Arrhenius plots (a) and Eyring plots (b) *versus* $1/T$ are shown in Fig. 5. The activation enthalpy and entropy were calculated from the fitted straight line and the values are listed in Table 4.

Table 2 Integral and differential forms of kinetic mechanism functions

| Function	Mechanism	Differential form $f(\alpha)$	Integral form
Parabolic rule	One-dimensional diffusion	$1/2\alpha$	α^2
Valens equation	Two-dimensional diffusion	$[-\ln(1 - \alpha)]^{-1}$	$\alpha + (1 - \alpha)\ln(1 - \alpha)$
Z–L–T equation	Three-dimensional diffusion	$\frac{3}{2}(1 - \alpha)^{4/3}[1/(1 - \alpha)^{1/3} - 1]^{-1}$	$[1/(1 - \alpha^{1/3}) - 1]^2$
Reaction order	Chemical reaction, $n = 0.5$	$(1 - \alpha)^{1/2}$	$2[1 - (1 - \alpha)^{1/2}]$
Reaction order	Chemical reaction, $n = 2$	$(1 - \alpha)^2$	$(1 - \alpha)^{-1} - 1$
Avrami–Erofeev equation	Nucleation and growth ($n = 2$)	$4(1 - \alpha)[-\ln(1 - \alpha)]^{3/4}$	$[-\ln(1 - \alpha)]^{1/4}$
Contraction ball (volume)	Phase boundary reaction, spherically symmetric	$3(1 - \alpha)^{2/3}$	$1 - (1 - \alpha)^{1/3}$
—	Autocatalytic reaction	$\alpha(1 - \alpha)$	$\ln \alpha - \ln(1 - \alpha)$
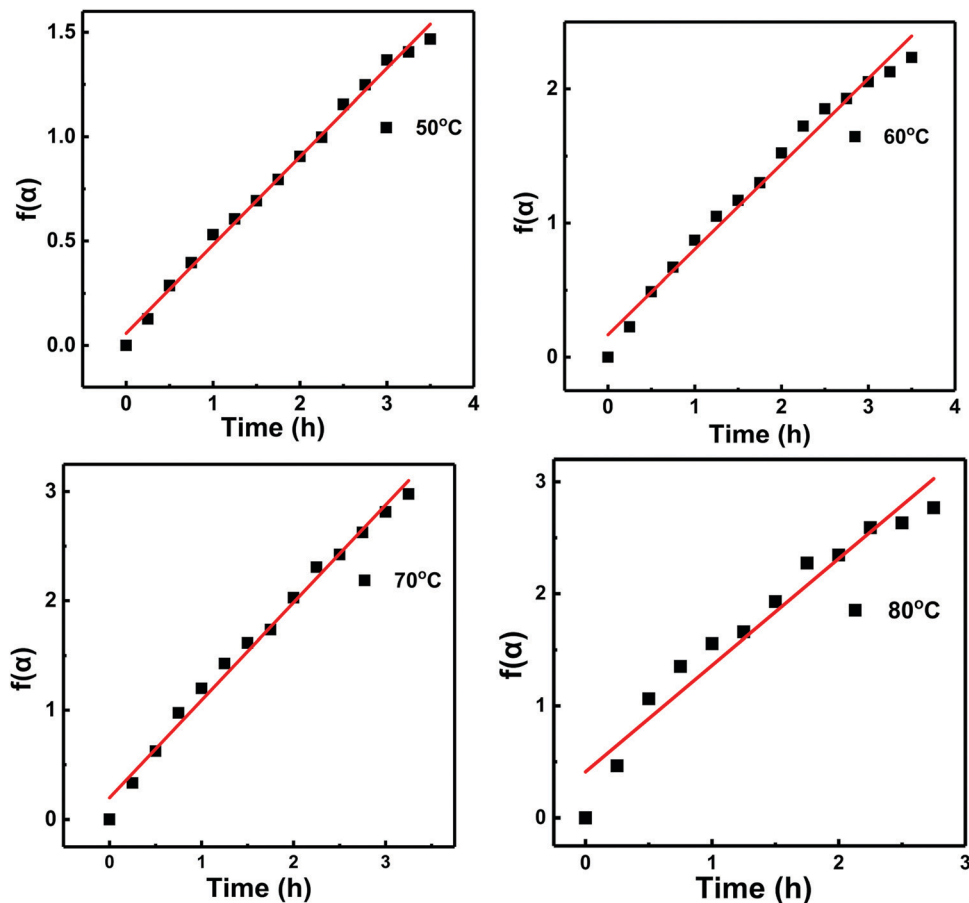
Fig. 4 $f(\alpha)$ vs. time linear fitting curves at different temperatures.

Table 3 The values of the fitted correlation coefficient r and the slope of the line k

Sample	Mechanism	r	k
DWPU-50	$\alpha/(1 - \alpha) = 0.423t + 0.058$	0.997	0.423
DWPU-60	$\alpha/(1 - \alpha) = 0.636t + 0.168$	0.992	0.636
DWPU-70	$\alpha/(1 - \alpha) = 0.893t + 0.197$	0.995	0.893
DWPU-80	$\alpha/(1 - \alpha) = 0.952t + 0.410$	0.972	0.952

3.4 Structural characterization of DWPUs

The FTIR spectra of DWPUs are shown in Fig. 6. The absorption bands corresponding to the stretching vibration of urea and carbamate groups could be observed at 3330 cm^{-1} (N–H) and 1705 cm^{-1} (C=O). The absorption bands at 1240 cm^{-1} and 1110 cm^{-1} were assigned to the stretching vibration of C–O in carbamate and ether groups, respectively. The absorption band from 2860 cm^{-1} to 2960 cm^{-1} was the stretching vibration of –CH$_2$ and –CH$_3$. These absorption peaks proved that WPU had been successfully synthesized. The absorption bands at 3469 cm^{-1} and 3428 cm^{-1} in the FTIR spectrum of DV26 were assigned to the stretching vibration of the primary amine, and the absorption band near 1400–1650 cm^{-1} was ascribed to the stretching vibration of the benzene group. As the concentration of DV26 increased, the vibration stretching absorption peak of benzene could be seen at 1490 cm^{-1}, which indicated that DV26 had

been successfully chemically bonded to the molecular chains of WPU.

The ^{1}H NMR spectra of DV26 and DWPU are shown in Fig. 7. The peaks at 7.26 ppm were attributed to the solvent CDCl$_3$. Other peaks of DV26 were listed as follows: 8.4 (m, 2H, Ar-H), 7.78 (dd, 2H, Ar-H), 7.26 (m, 4H, Ar-H), 7.08 (t, 2H, Ar-H), and 6.75(d, 4H, Ar-H). The signals assigned to benzene were observed in the ^{1}H NMR spectrum of DWPU, which indicated that DV26 had been anchored to the WPU chains.

3.5 Particle size, zeta potential, M_p and M_n

The particle size, zeta potential, M_p and M_n of the DWPUs are shown in Table 5. The particle size of DWPUs was significantly larger than that of WPU, and gradually increased as the concentration of DV26 increased. This was attributed to the introduction of hydrophobic DV26 which enhanced the hydrophobicity of WPU and affected the stability of the electric double layer. Owing to the poor compatibility between DV26 and WPU, the M_p of DWPU-25 was as high as 23.45%, and the particle size was the largest (50.16 nm). The low conversion of DV26 caused the precipitation of DWPU-50 emulsion after centrifugation. The results of the zeta potential and centrifugal stability test indicated that DWPU emulsions had good stability.

The percentage of migration (M_p) was used to evaluate the migration property of DWPU. M_p was one of the most important

Fig. 5   Arrhenius plots (a) and Eyring plots (b) *versus* 1/*T*.

Table 4   The values of activation enthalpy and entropy

Arrhenius law				Eyring equation			
Mechanism	r	E_a (kJ mol^{-1})	A (h^{-1})	Mechanism	r	ΔH (kJ mol^{-1})	ΔS (J (mol K)$^{-1}$)
$y = -2.816 \times x + 8.006$	0.972	23.41	2999	$y = -2.478 \times x + 1.184$	0.964	−20.60	−187.71

Fig. 6   FTIR spectra of DWPUs (a: DWPUs and b: a partially enlarged view of a).

parameters to evaluate dye performance. Compared with DWPU-25, D$_2$WPU exhibited excellent thermal migration properties with a M_p of only 4.43% (18.9% of DWPU-25). This could be attributed to the strong chemical bond between DV26 and the WPU molecular chain. In addition, as the reaction temperature increased, the final conversion of DV26 increased, which reduced the M_p of DWPU. As the concentration and the reaction temperature of DV26 increased, the content of the chain extender (DV26) reacting with WPU increased, eventually resulting in an increase in the M_n of DWPU.

3.6   Water resistance

Polymeric dyes are inevitably exposed to water during applications. The stability and service life of polymeric dyes with poor water resistance deteriorate seriously after contact with water. The water resistance of DWPUs was evaluated by measuring the water absorption rate and water contact angle. The water absorption rates of DWPUs decreased remarkably with the increase in concentration of DV26, while the contact angle increased significantly (Fig. 8). The introduction of hydrophobic DV26 into the WPU molecular chain could enhance the hydrophobicity of WPU. In addition, the urea group formed by the reaction of primary amino group with isocyanate could constitute more hydrogen bonding force, which could function as a physical crosslinking point. The combined effect of increasing hydrophobicity and hydrogen bonding forces made the water absorption rate decrease and the contact angle increase.
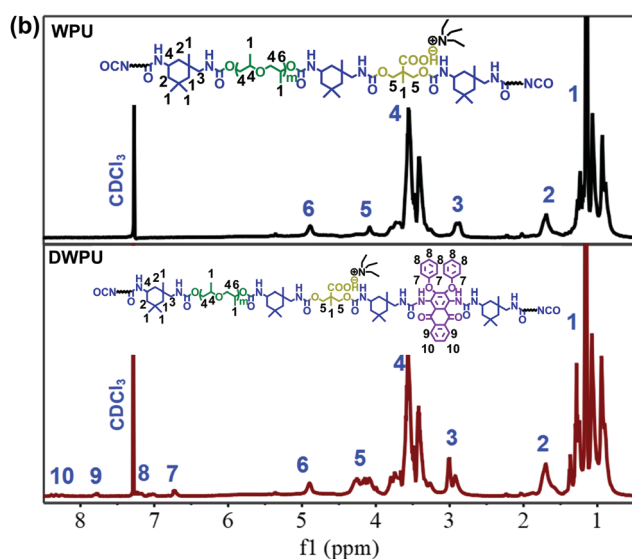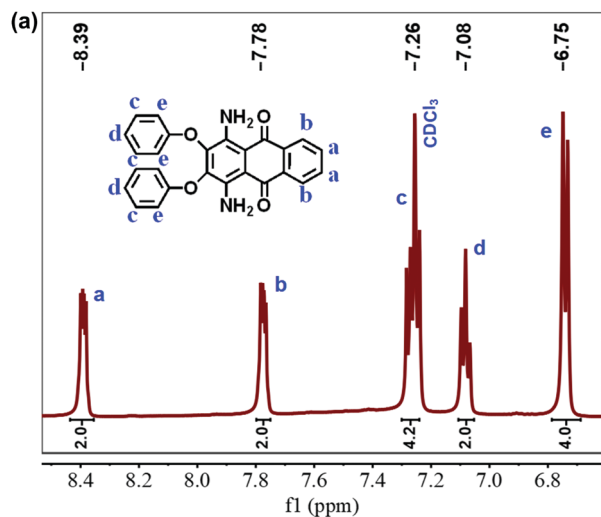
Fig. 8   Water absorption rate and water contact angle values of DWPUs.

Fig. 7 ^{1}H NMR spectra of DV26 (a) and DWPU (b).

Therefore, after DV26 was introduced, the water resistance of DWPU was greatly improved.

3.7   Thermal properties

Because the coloration of polymeric dyes must be carried out at high temperatures, thermal stability is a significant factor in
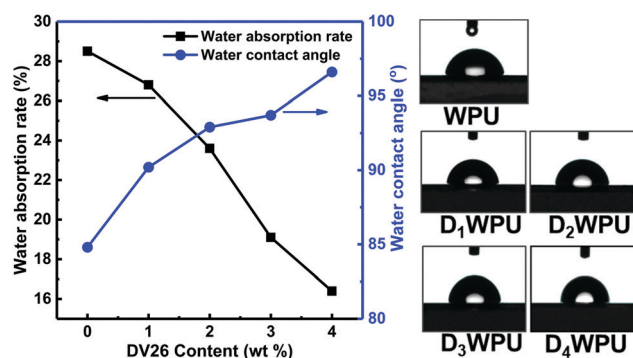
their performance for applications. The thermal properties of the flame-retardant polymeric dyes were evaluated using TGA, DTG and DSC (Fig. 9 and Table 6).

The thermal decomposition of WPU without the addition of DV26 was divided into two degradation stages.[35] The first stage was the decomposition of carbamate and urea groups in the hard segment, which occurred from 250 to 350 °C, with the maximum decomposition rate at 329.0 °C. The second stage between 350 and 420 °C was the decomposition of polyester in the soft segment, with the maximum decomposition rate at 370 °C. The char yield of WPU at 500 °C was only 0.9%. The pyrolysis process of DV26 had only one stage, which occurred in the range of 310–450 °C, and the maximum thermal decomposition temperature was 396 °C. The char yield of DV26 at 500 °C was as high as 9.3%. DV26 exhibited excellent thermal stability.

Due to the addition of DV26, more urea groups and hydrogen bonding were formed in the hard segment, which could improve the thermal stability of the hard segment in DWPUs. Moreover, the decomposition of the hard segment in DWPUs was delayed by DV26. Therefore, the thermal decomposition of DWPUs increased to three stages. The first stage between 250 and 280 °C was the decomposition of a part of the carbamate group in the hard segment, and the maximum degradation temperature was about 270 °C. The second stage was the decomposition of the remaining carbamate and urea groups in the hard segment, which occurred from 280 to 350 °C, with the maximum decomposition rate at 330 °C. The third stage between 350 to 420 °C was the decomposition of the soft segments, and the maximum decomposition temperature was

Table 5   Particle size, zeta potential, M_p and M_n values of DWPUs

Sample	Particle size/nm	Zeta potential/mV	Centrifugal stability	M_p/%	M_n	PDI
WPU	30.44	−32.1	No precipitate	—	25 100	1.90
DWPU-25	50.16	−29.3	Precipitate	23.45	25 900	2.58
DWPU-50	42.37	−30.0	Precipitate	6.53	27 700	2.41
DWPU-60	41.53	−31.8	No precipitate	4.62	29 100	2.25
DWPU-70	43.30	−33.1	No precipitate	4.27	30 200	1.98
DWPU-80	47.95	−31.9	No precipitate	4.22	31 000	2.05
D_1WPU	40.29	−37.2	No precipitate	3.79	29 400	2.04
D_2WPU	43.30	−33.1	No precipitate	4.27	30 800	1.97
D_3WPU	48.49	−36.6	No precipitate	4.43	32 200	2.07
D_4WPU	53.31	−34.7	No precipitate	4.62	33 500	2.12

Fig. 9 TGA (a), DTG (b) and DSC (c) curves of DWPUs.

Table 6 The thermal properties of DWPUs

Sample	$T_{5\%}$ (°C)	T_{1max} (°C)	T_{2max} (°C)	T_{3max} (°C)	Char yield (%)	T_{gs} (°C)	T_{gh} (°C)	ΔT_g (°C)
WPU	249.4	—	329.0	370.1	0.9	−43.6	92.9	136.5
D$_1$WPU	251.3	269.6	323.4	368.5	1.9	−44.3	94.2	138.5
D$_2$WPU	253.2	271.0	328.2	363.7	2.2	−44.6	97.4	142.0
D$_3$WPU	253.6	270.3	327.1	364.8	2.6	−44.9	100.3	145.2
D$_4$WPU	254.9	272.6	327.8	365.2	3.0	−44.1	103.8	147.9
DV26	309.7	—	—	396.4	9.3	—	—	—

365 °C. The char yield of D$_4$WPU at 500 °C was 3.0%, which was about 3 times that of WPU.

Because of the existence of micro-phase separation, WPU had two glass transition temperatures (T_g): the T_g of the soft segment (T_{gs}) and the T_g of the hard segment (T_{gh}). Generally, the difference value (ΔT_g) between T_{gs} and T_{gh} could be utilized to characterize the degree of micro-phase separation in WPU. With the increased content of DV26, the T_{gh} of DWPU shifted to higher temperatures and the ΔT_g increased from 136.5 to 147.9 °C. This indicated that the micro phase separation degree between the hard and soft segments enhanced, which was attributed to the stronger hydrogen bonding in the hard segment.

3.8 The properties of coated polyester fabrics

3.8.1 Color properties.
With the content of DV26 increasing, the content of the chromophore coated on fabric was increased. Therefore, the K/S value, a* and b* of coated fabric gradually increased, while the L* decreased by degree (Table 7),

Table 7 The color parameters of DWPU-coated polyester fabrics

Sample	Photograph	K/S	L*	a*	b*	c*	h^0
DWPU-25		1.77	58.16	25.87	−8.79	26.98	340.73
D$_1$WPU		1.397	61.66	22.94	−9.15	24.7	338.25
D$_2$WPU		2.370	54.96	27.29	−8.58	28.61	342.54
D$_3$WPU		3.792	49.55	34.39	−14.47	37.31	337.18
D$_4$WPU		4.939	46.31	36.1	−12.27	38.13	341.23

Table 8   The color fastness of polyester fabrics coated with DWPUs

Sample	Dry rub fastness	Wet rub fastness	Washing fastness
DWPU-25	4	3–4	3
D_1WPU	4–5	4–5	4
D_2WPU	4–5	4–5	4
D_3WPU	4–5	4–5	4
D_4WPU	4–5	4–5	4

Fig. 10   SEM micrographs of polyester fabrics (a) and fabrics coated with D_2WPU (b). The scale bars are 10 μm.

which indicated that the color of the coated fabric became deeper and deeper. Compared with the fabric coated with D_2WPU, the fabric coated with DWPU-25 exhibited a lower K/S value, a^* and b^*. The weak binding force between the polymer backbone and the DV26 physically blended in DWPU-25 resulted in a higher M_p, which eventually meant the fabric coated with DWPU-25 had a lighter color.

3.8.2   Color fastness. The color fastness (Table 8) showed that the dry rub fastness, wet rub fastness and washing fastness of polyester fabrics coated with DWPU-25 were 4 grade, 3–4 grade and 3 grade, respectively. However, those of fabrics coated with DWPUs were increased accordingly up to 4–5 grade, 4–5 grade and 4 grade. which was ascribed to the strong chemical bond between DV26 and the WPU chain. Therefore, fabrics coated with DWPUs would hardly fade during storage and use processes. While the dyes of the fabric coated with DWPU-25 were liable to fall off owing to the weak physical bonding forces.

3.8.3   Micrographs. The surface of the original polyester fabrics (Fig. 10a) showed natural grooves and characteristic parallel ridges. After coating with D_2WPU, the fabrics (Fig. 10b) showed a smooth and flat surface, which indicated that D_2WPU had been successfully coated on the surface of fabrics and had a good compatibility with polyester fabrics.

4. Conclusions

In this work, a series of polymeric dyes based on WPU were successfully synthesized. The utility of UV absorption spectroscopy for monitoring the polymerization of WPU-based polymeric dyes was highlighted. This simple method was equally applicable to other polymeric dye systems. The end of the reaction could be determined from a curve of conversion versus time. The results showed that DV26 could be completely reacted at 70 °C for 2.5 h. The reaction mechanism corresponded to the autocatalytic reaction equation, basically. Moreover, the properties of DWPUs

were characterized in detail. DWPUs exhibited good emulsion stability and M_p was only 4.43% (18.9% of DWPU-25). Due to the introduction of DV26, the thermal stability and water resistance of DWPUs were greatly improved. In the end, DWPUs were applied to polyester fabric coatings and showed excellent application properties.

Conflicts of interest

The authors declare no competing financial interests.

Acknowledgements

References

1 T. C. Wen and Y. J. Wang, Ind. Eng. Chem. Res., 1999, 38, 1415–1419.
2 Y. Cheng, L. Wei, Z. Li, R. Zhang, H. Wen, G. Bo, G. Chen, G. Ping, M. M. F. Yuen and C. P. Wong, Adv. Funct. Mater., 2011, 21, 4582–4588.
3 V. García-Pacios, J. A. Jofre-Reche, V. Costa, M. Colera and J. M. Martín-Martínez, Prog. Org. Coat., 2013, 76, 1484–1493.
4 M. Elgammal, S. Prévost, R. Schweins, R. Schneider and M. Gradzielski, Colloid Polym. Sci., 2014, 292, 1487–1500.
5 H. H. Wang and I. S. Tzun, J. Appl. Polym. Sci., 2015, 73, 245–253.
6 H. Sardon, L. Irusta, M. J. Fernándezberridi, M. Lansalot and E. Bourgeatlami, Polymer, 2010, 51, 5051–5057.
7 E. C. Buruiana and T. Buruiana, Eur. Polym. J., 2001, 37, 2505–2511.
8 M. Beija, M. T. Charreyre and M. G. J. Martinho, Prog. Polym. Sci., 2011, 36, 568–602.
9 B. Jang, S. Y. Kim and J. Y. Do, Dyes Pigm., 2012, 94, 217–223.
10 Z. Chang, M. Zhang, A. G. Hudson, E. B. Orler, R. B. Moore, G. L. Wilkes and S. R. Turner, Polymer, 2013, 54, 6910–6917.
11 C. T. Huang and K. N. Chen, J. Appl. Polym. Sci., 2010, 100, 1919–1931.
12 Z. Ge, W. Li and Y. Luo, Eur. Polym. J., 2009, 45, 530–536.
13 H. Mao, C. Wang and Y. Wang, New J. Chem., 2015, 39, 3543–3550.
14 X. Hu, X. Zhang, J. Dai and J. Liu, J. Lumin., 2011, 131, 2160–2165.
15 S. Shang, K. L. Chiu and S. Jiang, J. Appl. Polym. Sci., 2017, 134, 44710.
16 S. Sami, E. Yildirim, M. Yurtsever, E. Yurtsever, E. Yilgor, I. Yilgor and G. L. Wilkes, Polymer, 2014, 55, 4563–4576.
17 X. Hu, X. Zhang, J. Liu and J. Dai, Polym. Int., 2014, 63, 453–458.
18 X. Hu, X. Zhang, J. Liu and J. Dai, J. Lumin., 2013, 142, 23–27.
19 I. Yilgör, E. Yilgör and G. L. Wilkes, Polymer, 2015, 58, A1–A36.
20 H. Sardon, J. M. W. Chan, R. J. Ono, D. Mecerreyes and J. L. Hedrick, Polym. Chem., 2014, 5, 3547–3550.
21 D. Filip and S. Vlad, Polym. Int., 2015, 63, 1944–1952.

22 G. A. Alvarez, M. Fuensanta, V. H. Orozco, L. F. Giraldo and J. M. Martín-Martínez, *Prog. Org. Coat.*, 2018, **118**, 30–39.

23 J. Su, Y. Yan, Y. Chen, X. Zeng, H. Xiang, Y. Cui and X. Liu, *Prog. Org. Coat.*, 2018, **119**, 76–84.

24 J. Gu, H. Gu, C. Jin, S. Chen, L. Ni and X. Jie, *Appl. Surf. Sci.*, 2018, **439**, 589–597.

25 H. Mao, F. Yang, C. Wang, Y. Wang, D. Yao and Y. Yin, *RSC Adv.*, 2015, **5**, 3631–3639.

26 C. Zhou, T. Xie, R. Zhou, C. O. Trindle, Y. Tikman, X. Zhang and G. Zhang, *ACS Appl. Mater. Interfaces*, 2015, **7**, 17209–17216.

27 N. I. Sakellarios and S. G. Kazarian, *J. Chem. Thermodyn.*, 2005, **37**, 621–626.

28 D. H. Yong, F. Y. Peng, J. Y. Li, D. Q. Cong and D. L. Tian, *React. Kinet., Mech. Catal.*, 2010, **101**, 41–48.

29 C. Chai, J. Hou, X. Yang, G. Zheng, M. Huang and G. Li, *Polym. Test.*, 2018, **69**, 259–265.

30 L. Mashlyakovskiy, E. Khomko, V. Zaiviy and C. Tonelli, *J. Polym. Sci., Part A: Polym. Chem.*, 2015, **38**, 2579–2602.

31 F. Schapman, J. P. Couvercelle and C. Bunel, *Polymer*, 1998, **39**, 4955–4962.

32 A. A. Caraculacu and S. Coseri, *Prog. Polym. Sci.*, 2001, **26**, 799–851.

33 K. Hailu, G. Guthausen, W. Becker, A. König, A. Bendfeld and E. Geissler, *Polym. Test.*, 2010, **29**, 513–519.

34 S. K. Rath, A. M. Ishack, U. G. Suryavansi, L. Chandrasekhar and M. Patri, *Prog. Org. Coat.*, 2008, **62**, 393–399.

35 W. Gang, J. Li and Y. Luo, *Polym. Degrad. Stab.*, 2016, **123**, 36–46.